2-D deployment of aerial base stations: a simulation model to provide voice communication

Gabriela Rodríguez-Cortés[a], Anabel Martínez-Vargas[a,*], MA Cosío-León[a], Daniela M. Martínez[b], Oscar Montiel[c]

[a] *Universidad Politécnica de Pachuca, Carretera Pachuca - Cd. Sahagún km 20, Zempoala, 43830, Hidalgo, México*
[b] *Facultad de Ciencias de la Ingeniería y la Tecnología, Universidad Autónoma de Baja California, Blvd. Universitario 1000, Tijuana, 21500, Baja California, México*
[c] *Instituto Politécnico Nacional - CITEDI, Ave. Instituto Politécnico Nacional 1310, Tijuana, 22435, Baja California, México*

Abstract

Unmanned aerial vehicles (UAVs) offer a potential alternative for providing voice services in areas where communication is disrupted due to natural disasters. These UAVs can be configured as aerial base stations (ABSs), enabling the deployment of a temporary communications network. However, communication networks based on ABSs pose several significant challenges. One of these challenges involves addressing interruptions or limitations in network coverage caused by natural disasters. In such situations, there is a high likelihood that users within the affected area may be unable to communicate due to a lack of coverage. This is a complex problem because it depends on factors, such as the mobile user locations, the characteristics of the air-to-ground channel, and geographical details of the area. In this work, we propose an optimization model to determine the placement of a set of ABSs within a limited disaster area that maximizes the probability of successful voice services (PSVSs). This optimization model integrates a network evaluation model that analyzes the wireless environment at a specific time. The network evaluation model utilizes two-ray and Rayleigh channel models, enabling the simulation of a worst-case scenario for wireless communication systems. We evaluate the proposed optimization model using the (1+1)-evolution strategy with a one-fifth success rule. We explore various

*Corresponding author

parameter configurations to understand their impact on algorithm performance. This analysis helps identify the configuration of the optimization model that yields the maximum PSVSs. Simulation results indicate that by appropriately configuring the evolution strategy algorithm and comparing random ABS locations with those determined ABS locations by the evolution strategy algorithm, the PSVS can be enhanced by an average of 60%.

Keywords:
UAV placement problem, aerial base stations, multi UAV deployment, evolution strategy

---

1. Introduction

Human-induced climate change increases the frequency of natural disasters [1]. According to [2], natural disasters are classified as land-based (e.g., earthquakes), water-based (e.g., river floods), atmospheric (e.g., tornadoes), biological (e.g., pandemics), extraterrestrial based (e.g., comet strikes), or even a combination of them (e.g., undersea earthquake and tsunami). Although different, they indistinctly cause loss of life and damage to humans and their possessions. Search and rescue operations involve a series of actions that occur during the response phase of a natural disaster, to provide aid to the potentially injured population. These activities are carried out by trained first responders, including firefighters, paramedics, and emergency personnel. One of the main requirements for these first responders to effectively carry out search and rescue operations is to have a reliable communications network. However, it is possible that the regular communications infrastructure may be partially damaged or destroyed as a consequence of the natural disaster. Therefore, in such critical circumstances, an adaptable, reconfigurable, easily deployable, and reliable communications network is essential. Due to flexible deployment, low cost, and rapid reconfiguration, unmanned aerial vehicles (UAVs) are the most suitable candidates for deploying a temporary wireless network [3]. In this way, UAVs can serve as temporary aerial base stations (ABSs) and dynamically change their location to provide on-demand communications to the first responders and victims on the ground in a natural disaster [4]. For example, in Puerto Rico, AT&T deployed its helicopter Flying COW (Cell on Wings) to connect residents temporarily and first responders after Hurricane Maria's devastation [5].

Despite the above, as the work in [3] mentions, there are several challenges to efficiently deploying an ABSs-based wireless network. Some of the main concerns in such deployment are ABS placement, resource management, interference management, and channel modeling. UAV placement is one of the biggest challenges since it depends on the location of a mobile user, air-to-ground channel characteristics, geographical area details, and energy constraints of UAVs. The optimization problem of finding the best position of ABSs to maximize the network performance is an NP-hard problem [6]. Also, UAV position directly impacts the performance metrics of a communication network, like signal-to-interference and noise ratio (SINR). This performance metric depends on the transmitter and receiver's location and distance, the transmission power, and the characteristics of the radio channel. Therefore, ABS placement impacts the quality of service (QoS) perceived by mobile users when they intend to access the network to request services. Addressing these challenges associated with deploying ABS-based wireless networks is imperative to ensure efficient network operation and deliver quality services to mobile users.

This paper contributes to state-of-the-art with an optimization model that incorporates a network evaluation model. Regarding the optimization model, we have proposed an objective function that maximizes the probability of successful voice services according to the suitability of locations to deploy the ABSs on a 2D city map. The above is constrained to locate ABSs within the bounds of the disaster zone. The integrated network evaluation model into the optimization model analyses the network at a given instant time. To do so, we capture a 5G wireless environment within a disaster area where the base stations collapsed (due to the natural disaster) and the mobile users (victims and first responders) need to communicate. In this process, the ABSs' channels are assigned to mobile users according to propagation conditions modeled using Rayleigh and two-ray channel models. These models simulate challenging signal propagation conditions to ensure quality voice service in critical circumstances.

It is recognized that determining the optimal 3D placement of UAVs involves complex mathematical modeling and advanced optimization techniques. These strategies are often computationally intensive, particularly in real-time applications. To reduce the complexity associated with 3D deployment, several studies like [7, 8, 9] have proposed decoupling the 3D UAV deployment into two dimensions: vertical and horizontal. In [7], the horizontal dimension is focused on determining UAV locations, while the vertical

dimension is concerned with altitude optimization. The UAV altitude affects the cell radius and the path loss experienced within the cell, while the horizontal location and cell radius determine the ground users covered by the UAVs. In contrast, the study in [8] addresses the calculation of the optimal horizontal deployment coordinates of the UAVs. Subsequently, in the vertical dimension, the authors determine the transmission power and deployment height of the UAVs. Finally, in [9], the authors aim to maximize the number of covered users in the horizontal dimension by utilizing the minimum required transmission power in the vertical dimension. While these approaches successfully reduce deployment complexity by dividing the problem into two dimensions, they simultaneously address two distinct optimization problems. Consequently, the solutions remain computationally demanding, making it challenging to provide feasible solutions faster. Even though our primary analysis framework is 2D, the UAV's height is not neglected; rather, it is a built-in aspect of the channel model that influences propagation characteristics. This is consistent with the focus of our study: to provide a practical, computationally efficient, and accurate assessment of UAV-based communication in disaster scenarios without the need for a full 3D model.

Nowadays, data transmission has become increasingly popular in modern communication. This service offers significant advantages, including faster communication and more efficient data usage. However, it may not be the most suitable option in emergency scenarios due to its reliance on specific infrastructure and technologies. For example, data service requires greater bandwidth and spectral resources, which could be a limitation in emergency scenarios where such resources are scarce or unavailable. Additionally, bandwidth limitations may arise in areas with network congestion, such as during natural disasters or large-scale events, which could deteriorate call quality and hinder effective communication. On the other hand, classic voice transmission in mobile networks uses proven technologies such as LTE, which may be more robust in emergencies where terrestrial infrastructure has been destroyed. This technology has been tested over time and has proven to provide reliable communication even in challenging conditions. Furthermore, classic voice transmission has a greater availability of compatible devices. This simplicity can be advantageous in emergencies where a quick and efficient response is needed without relying on complex systems that may be prone to failure.

We apply the (1+1)-evolution strategy ((1+1)-ES) with a one-fifth suc-

cess rule [10] to locate ABS in the affected area. (1+1)-ES is inspired by biological evolution dating back to the 1960s. It is mainly applied to solve optimization problems in continuous search spaces [11]. It generates one offspring from one parent in each generation, mimicking the asexual reproductive mechanism of biological evolution. Subsequently, the parent and offspring are compared to designate the fittest individual as the parent for the next generation. The genetic algorithms (GAs) use a similar process of evolution. However, (1+1)-ES offers distinct advantages over GAs, particularly its ability to yield high-quality solutions with minimal objective function evaluations and using small population sizes compared to GAs. Additionally, (1+1)-ES can self-adjust mutation rates through the one-fifth success rule in each generation [10]. These features render (1+1)-ES highly suitable for rapidly generating solutions in natural disaster scenarios when compared to GAs.

To imitate the non-availability of internet support because of infrastructure failure (thus no access to cloud computing services), we run the optimization model, the (1+1)-ES, and the snapshot-network evaluation on NVIDIA's Jetson TX2. This device is part of edge artificial intelligence (AI), a technology where AI algorithms are processed on edge. Thus, in an emergency situation, one of the UAVs will be an AI UAV, this is, a UAV running with edge AI. Once the (1+1)-evolution strategy produces the optimal placement of UAVs to maximize the probability of successful voice services, the AI UAV communicates to all the UAVs in the temporal network their new locations. The communication protocol necessary to do the above task is outside the scope of the present work.

1.1. Related Works

Several studies attempt to find positions for the ABSs to meet different objectives. For example, the work in [4] uses a drone's edge device (jetson nano) to take aerial video that is the input to the image classifier model. Then, the authors apply a convolutional neural network to detect survivors; when the model detects the survivor, the drone hovers over the survivor to provide access to the wifi network with an accuracy of 94%. However, the authors did not perform an evaluation analysis of the network conditions for reliable communication. On the other hand, work in [12] evaluates the network performance of UAV-assisted intelligent edge computing to search and rescue missions. It considers network parameters such as delay, throughput,

traffic sent and received, and path loss. It also proposes a model to detect people in a localized area using a convolutional neural network. When the UAV computing-based surveillance system identifies the survivor's position, their position is given to the search and rescue team for assistance. The authors use OPNET to create the evaluation scenario. Their evaluation scenario is limited to two UAVs.

Likewise, work in [13] minimizes the number of UAVs deployed in a disaster area to provide communication and the total distance flown by UAVs to restore connectivity. Each UAV uses the angle of arrival (AoA) and the received signal strength indicator (RSSI) to estimate the number of nodes in the jth disconnected part. Simultaneous movement of multiple UAVs to locate them in the affected area to recover communication is not allowed. The above is critical since the time to recover connectivity cannot be sped to save lives. Furthermore, even if this work uses the term "minimize," it does not imply it addresses an optimization problem. In contrast, work in [14] addresses the 3D location problem of multiple ABSs. It also allocates resources to mobile users, maximizing the network's profit (from the service providers' perspective). It applies the modified-alternate location-allocation (M-ALA) heuristic that alternately solves two sub-problems: a bandwidth allocation sub-problem, and the location sub-problem of the ABSs. Their largest instance has 5000 users, while our proposed instance has 19819 mobile users.

The work in [15] poses the ABSs placement as an optimization problem to determine the number and location of the ABSs to provide connectivity in flash crowds and emergencies. It considers the position of the ground users, mobile user channel quality, and the positions of the other ABSs. The above information feeds a genetic algorithm that finds the minimum number of ABSs to connect to mobile users. The authors report 90% of connected users for 55 mobile users. They consider WiFi to recover the communication between ABSs and mobile users. Their instance size of 55 mobile users does not capture the high concentration of users that a disaster area could have. A study in [16] compares five placement algorithms to minimize the number of ABSs to guarantee a minimum rate for mobile users in an urban environment. These five placement algorithms are circle-based placement based on a sparse-recovery optimization approach, clustering-based positioning at a fixed altitude, circle-based positioning based on an inward spiral around the uncovered mobile users, 3D positioning via empirical models, and 3D placement using radio maps. Among those algorithms, 3D placement using radio

maps is the one that performs better. The above is because of its awareness of the path loss in the area. Its simulations include up to 90 mobile users in the area.

The authors in [17] maximize the mean opinion score (MOS) through the 3D UAVs' placement and dynamic movement. To do so, they apply a genetic algorithm based on the k-means (GAK-means) algorithm to generate the cell partition of the users. After that, they use a Q-learning algorithm to move UAVs in seven flying directions. Their signal model includes the line-of-sight (LoS), the non-line-of-sight (NLoS) probability, the SINR, and the quality of experience (QoE). Their simulation has 100 ground users and four UAVs. They conclude that their proposed scheme outperforms the k-means and the iterative-GAKmean (IGK) algorithms. In [18], the authors presented a model to maximize network throughput. First, the SINR is calculated in mobile users; then, the authors apply the artificial bee colony (ABC) algorithm to find a good solution. Results show that ABC solves the problem of network throughput optimization and finds the optimal flight position of the ABSs.

Table 1 summarizes the key findings of each work discussed above in the UAV placement problem. These works do not address the ABS placement problem as one of maximizing the probability of successful voice services. We propose this objective function to guarantee that once the (1+1)-ES finds the strategic locations of the ABSs, the temporal wireless network supports the highest number of successful voice services among the first responders and victims. It is important to note that those successful voice services are provided with QoS. We prioritize the provision of this basic 5G mobile service because it requires less bandwidth than data and video services. Additionally, real-time voice transmission often requires lower latency than data and video services. Voice communication can be more accessible to users with limited bandwidth or older devices that may not support high-definition video streaming. This simplicity can result in lower hardware and software requirements, as well as reduced energy consumption. These characteristics can be advantageous in emergency scenarios, providing essential communication capabilities without incurring high infrastructure costs and preventing performance degradation of the temporary wireless network.

Furthermore, our proposed optimization model verifies that the positions for the ABSs are kept within the bounds of the affected zone. Also, we have different mobile user statuses: present, requesting, candidate, and served. Mobile user statuses determine how users interact and evolve with the tem-

Type of UAV placement	Objective	Algorithm(s)
Single UAV placement [4]	Survivors detection	Convolutional neural network
Multi UAV deployment [12]	Survivors detection	Convolutional neural network
Multi UAV deployment [13]	Minimizing the number of ABSs, minimizing distance flown by ABSs	Heuristic
Multi UAV deployment [14]	Maximizing the profit of the network	Heuristic
Multi UAV deployment [15]	Minimizing the number of ABSs to provide connectivity	Genetic algorithm
Multi UAV deployment [16]	Minimizing the number of ABSs to guarantee a minimum rate at mobile users	Circle-based placement, clustering-based placement, 3D placement via empirical models, 3D placement using radio maps
Multi UAV deployment [17]	Maximizing the mean opinion score (MOS)	Genetic algorithm based on the k-means (GAK-means), Q-learning algorithm
Multi UAV deployment [18]	Maximizing network throughput	Artificial bee colony (ABC) algorithm

Table 1: Summary of the related work on the objectives and the optimization techniques used for ABS placement.

poral wireless network. To obtain a new status, the mobile user must comply with a set of requirements. In this sense, the requirement to obtain a candidate status establishes that one mobile is linked to just one ABS. The above allows us to manage somehow the coverage radius overlapping among ABSs. In this way, the ABSs can cover a wide area of the affected area, which results in more mobile users with voice service.

Also, we generate an instance (see `https://figshare.com/articles/dataset/RC_CMU-PCP-19819_GZ/24194529`) that utilizes real geographic coordinates for mobile users and the boundaries of the affected disaster zone. These coordinates are sourced from Tula Town in Mexico, where in September 2021, the Tula River overflowed, resulting in the loss of voice and data services for 18 towns.

Finally, as opposed to the works discussed above, we apply the (1+1)-ES that allows us to directly use the ABS positions in geographical coordinates in the candidate solutions. Since the (1+1)-ES deals with one parent producing one offspring in each iteration, we can speed up the time to obtain a good solution, saving human lives. Also, the (1+1)-ES allows processing larger instance sizes than the ones reported by the works discussed above.

This article is organized as follows: Section 2 describes the simulation scenario, the snapshot-network evaluation, and the optimization model. Section 3 presents the (1+1)-ES to locate ABSs. Section 4 illustrates the simulation results. Finally, Section 5 concludes this study along with future directions.

2. Problem formulation

This section describes the simulation scenario. We also explain the network model for providing voice service to mobile users within the affected zone. Finally, we show the optimization model that determines the locations of each available ABS such that most mobile users attempting to make a

call can access the network with successful voice communication during the emergency.

2.1. Simulation scenario

We consider a simulation scenario in which we evaluate the optimization model proposed for representing the locations of ABSs that provide the maximum number of voice communication services after a natural disaster. We bound the square-shaped affected area of L meters per side, centered in latitude 20.033608 and longitude -99.319219. We assume that emergency services have a set $M = \{m_i\}$ of ABSs available for fast deployment, building a temporary cellular network. m_i is the geographic location of each ABS, that is $m_i = (x_i, y_i)$, such that $1 \leq i \leq |M|$, where $|M|$ is the cardinality of the set M. It is further assumed that ABSs have technological capabilities and functionalities to operate as ABS-LTE eNodeB suitable for voice services. LTE stands for Long-Term Evolution and is the technology proposed by the 3rd Generation Partnership Project (3GPP) to enable emergency connectivity using ABSs [19]. On the other hand, the set denoted by $N = \{n_j | n_j = (x_j, y_j)\ where\ x_{min} \leq x_j \leq x_{max}\ and\ y_{min} \leq y_j \leq y_{max}\}$ corresponds to the present mobile users (MUs) located inside the affected area, where $1 \leq j \leq |N|$. $|N|$ is the cardinality of the set N. $[x_{min}, x_{max}]$ is the bound in the latitude of the affected area. $[y_{min}, y_{max}]$ is the bound in the longitude of the affected area. The location of each MU is considered a random variable that follows a Poisson cluster process (PCP). PCP models a network where MUs cluster in line with certain social behavior [20], i.e., the PCP represents the MUs gathered around an inactive base station because of the natural disaster. Furthermore, some MUs become requesting mobile users (RMUs) because the MUs request a radio channel to initiate voice service. RMUs are represented by the set K, therefore $K \subseteq N$, then $K = \{k_j | n_j \in N\ and\ it\ requests\ voice\ service\}$. The selection of MUs to become RMUs is random and follows a uniform distribution. We also assume each available ABS knows the position of the MUs and RMUs within the disaster area. Figure 1 shows the simulation scenario of this work. The black lines represent the affected area bounds. The red triangles represent the set of ABSs the first responders have for strategically deploying. The scenario shown in Figure 1 has 19 819 MUs (blue circles), from which 4492 are RMUs (green circles).

The network performance evaluation, i.e., the number of RMUs properly attended, is analyzed by capturing the state of the network (snapshot) during

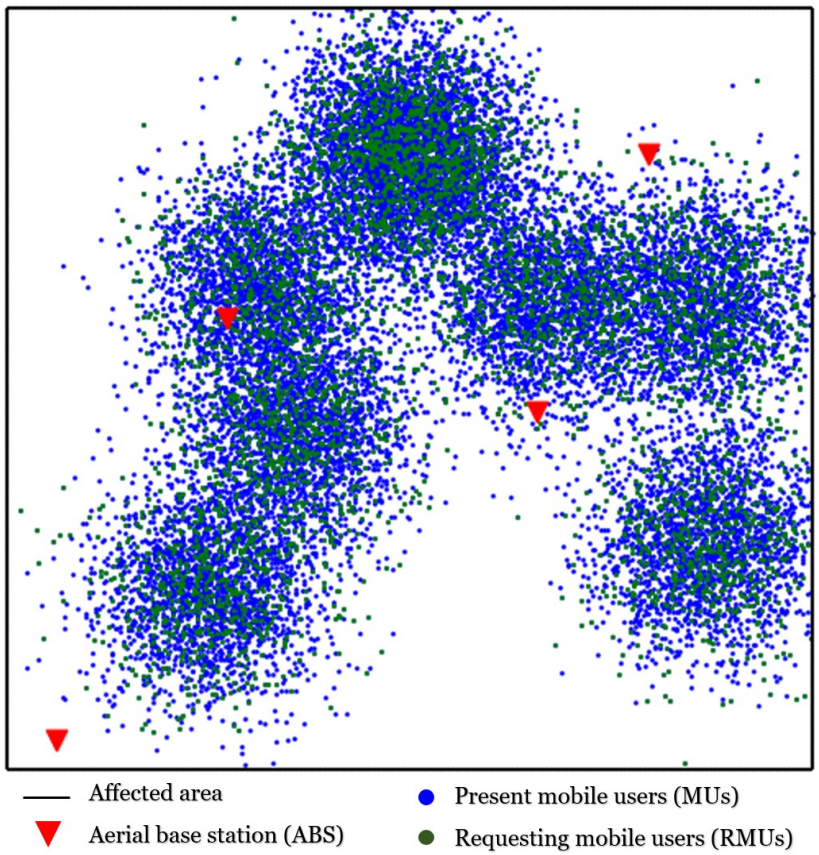

Figure 1: Simulation scenario proposed to locate ABSs in zones where communication services are interrupted.

a specific time. This can be considered as watching a movie film by observing cinematic snapshots and then collecting all the necessary information from each snapshot to understand the story told by the movie. During each snapshot, the number and positions of the mobile users remain constant for evaluation; however, the number of RMUs changes according to the dynamics of the Erlang traffic model. The snapshot-network evaluation determines the number of RMUs served by available ABSs. Performance evaluation is carried out by analyzing the communication link established from the ABS to the RMU, regarded as downlink communication analysis; this is the link with the most significant communication losses in the communication network design.

2.2. Snapshot-network evaluation

To evaluate every snapshot, we designed a network model based on LTE technology broadband in the 700 MHz frequency assigned to public safety communications (PSC), with 20 MHz of dedicated spectrum available for broadband, 10 MHz for downlink, and 10 MHz for uplink in band class 14 [19]. Since radio resources can be limited during an emergency, we guarantee only voice services for the RMUs. The 3GPP standardizes the voice service to 8 kHz [21]. In addition, given that the frequency division duplexing (FDD) scheme is considered; it requires two radio channels to establish a communication link, one to transmit and one to receive information. Then, the amount of available channels in the system is $\frac{10000\ kHz}{(8\ kHz \times 2}) = 625$ channels, i.e., the system has 625 available channels to provide communication to the victims. The channels are allocated to the RMUs according to a fixed channel assignment strategy. Table 2 lists the notations used in this paper.

Each ABS has a channel pool to serve the RMUs. However, an ABS can allocate a channel to an RMU only if the RMU becomes a candidate mobile user (CMU). A CMU must fulfill the following:

$$d_{m_i k_j} \leq 2\ km \tag{1}$$

$$\bigcap_{i=1}^{|M|} A_i = \emptyset \tag{2}$$

$$SINR_{k_j} \geq 3\ dB \tag{3}$$

Equation (1) represents the k_j within the coverage radius of the m_i. The coverage radius equal to two km was defined according to previous experiments. These prior experiments suggested that the interference can be reduced by setting the coverage radius equal to two km. The geographic distance between the k_j and the m_i is computed through the Haversine formula [22] given by:

$$d_{m_i k_j} = 2R \operatorname{atan2}(\sqrt{a}, \sqrt{1-a}) \tag{4}$$

where R is the radius of the earth. a is a value that considered two coordinates in latitude and longitude on the earth; it is given by:

$$a = \sin^2 \frac{x_i - x_j}{2} + \cos x_i \cos x_j \sin^2 \frac{y_i - y_j}{2} \tag{5}$$

where x_i and x_j are the m_i and the k_j latitudes, respectively; y_i is the longitude of the m_i, and y_j is the longitude of the k_j. where x_i and x_j are the m_i

Notation	Description
M, N	Set of the geographic coordinates of the available ABSs and MUs
m_i, n_j, m_q	Geographic coordinates of the available ABSs, MUs, and interfering signals, respectively
$\|M\|$, $\|N\|$	Number of available ABSs and MUs
K, k_j, $\|K\|$	Set of the geographic coordinates of the RMUs, geographic coordinates of the RMUs, and number of RMUs, respectively
$d_{m_i k_j}$, $d_{m_q k_j}$	Distance of desired signal and distance interfering signal, respectively
A_i	Set of CMUs that ABSs may allocate a radio channel
$SINR_{k_j}$	Signal-to-interference and noise ratio in one RMU
$Prx_{m_i k_j}$, $Prx_{m_q k_j}$	Received power of desired signal and interfering signals, respectively
$I_{m_q k_j}$	Power of interference at the RMU receiver in the desired signal
P_{tx}	Transmission power of the ABSs
$Pt_{m_i k_j}$, $Pt_{m_q k_j}$	Path-loss power in desired signal and interfering signals
$Pd_{m_i k_j}$, $Pd_{m_q k_j}$	Loss power by multi-path fading on the desired signal and interfering signals
U_i	Set of geographic coordinates of SMUs by one ABS
Γ	Number of SMUs properly attended
P_{BT}	Total blocking probability in the system
P_{BC}	Blocking probability due to coverage
P_{BR}	Blocking probability due to spectral resources
P_R	Call request probability
P_{OC}	User-out-of-coverage probability
P_{IC}	User-in-coverage probability
P_{NA}	Probability of non assignment

Table 2: Notations of the system model.

and the k_j latitudes, respectively; y_i is the longitude of the m_i, and y_j is the longitude of the k_j.

Equation (2) ensures that the k_j connects only to one m_i, where A_i is the set of CMUs linked to m_i. Equation (2) allows us to manage somehow the radius coverage overlapping among ABSs.

Equation (3) computes the single-hop communications metric. The SINR measures how much a desired signal is affected by other cells that use the same set of frequencies. It indicates that the receiver of the desired signal must achieve a minimum SINR threshold to represent a successful reception. The threshold in Equation (3) guarantees the successful provision of voice service in the LTE technology [23]. We evaluate the SINR caused by co-channel interference (CCI) [24], which is calculated by:

$$SINR_{k_j}(dB) = Prx_{m_i k_j}(dB) - I_{m_q k_j}(dB) \tag{6}$$

where $Prx_{m_i k_j}$ is the received power from the m_i to the k_j, i.e., the desired signal. $I_{m_q k_j}$ is the sum CCI power at the k_j receiver of the desired signal. CCI occurs when multiple ABSs share the same channel pool simultaneously [24]. Then to each receiver of the desired signal, the other ABSs appear to be interfering signals. For example, in Figure 2, m_q is the interfering signal of the k_j receiver of the desired signal. So m_q is the q-th interfering signal where $1 \leq q < |M|$ for all $q \neq i$. The CCI is expressed as:

$$I_{m_q k_j}(dB) = \sum_{q=1}^{|M|} Prx_{m_q k_j}(dB) \tag{7}$$

where the received power of the desired signal $Prx_{m_i k_j}$ and the received power of the interfering signal $Prx_{m_q k_j}$ are expressed as:

$$Prx_{m_i k_j}(dB) = P_{m_i}(dB) - Pt_{m_i k_j}(dB) - Pd_{m_i k_j}(dB) \tag{8}$$

$$Prx_{m_q k_j}(dB) = P_{m_q}(dB) - Pt_{m_q k_j}(dB) - Pd_{m_q k_j}(dB) \tag{9}$$

The received powers are modeled using the channel models: Rayleigh and two-ray. These models have been selected to capture the characteristics of the communication channel. The Rayleigh channel model simulates non-line-of-sight multipath fading and is often considered a worst-case scenario for wireless communication systems. In such circumstances, transmitted signals are expected to experience significant fading in both the uplink and downlink directions. The presence or absence of obstacles in a radio environment

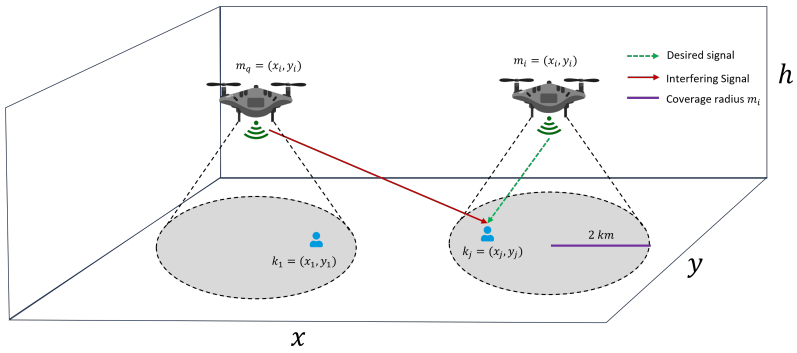

Figure 2: Approach to calculating SINR. m_i emits the desired signal to k_j receiver, m_q emits an interfering signal for the k_j receiver of the desired signal.

can be effectively modeled by theoretical random variables, eliminating the need to simulate the objects or obstacles themselves. Theoretical channel models such as Rayleigh, Rician, and k-Nakagami, among others, encompass the randomness associated with signal blockages, shadowing, moving objects, and other potential scatterers, all of which contribute to the total fading experienced by a received signal [25]. The two-ray channel model, on the other hand, provides a simplified representation of the communication environment, incorporating direct and reflected paths; it also has large accuracy for predicting large-scale signal strength over several kilometers for mobile radio systems [24]. Unlike the Rayleigh model, which accounts for multipath fading due to scattering, the two-ray model considers a direct line-of-sight path alongside a single reflected path. This model is particularly useful in scenarios where a clear line of sight exists between the transmitter and receiver, allowing for a more straightforward analysis of signal propagation characteristics. In Equations (8) and (9), $Pt_{m_i k_j}$ is the path-loss in the desired signal, and $Pt_{m_q k_j}$ is the path-loss in the interfering signal caused by the two-ray model. Consequently, $Pd_{m_i k_j}$ and $Pd_{m_q k_j}$ represent the fading in the desired signal and the interfering signal, respectively, caused by the Rayleigh model [26].

The path losses of the two-ray model for the desired signal and the interfering signal are given by:

$$Pt_{m_i k_j}(dB) = 40 \log d_{m_i k_j} - (10 \log G_{m_i} + 10 \log G_{k_j} + 20 \log h_{m_i} + 20 \log h_{k_j}) \tag{10}$$

$$Pt_{m_q k_j}(dB) = 40 \log d_{m_q k_j} - (10 \log G_{m_q} + 10 \log G_{k_j} + 20 \log h_{m_q} + 20 \log h_{k_j}) \quad (11)$$

where G_{m_i} is the gain of the antenna m_i and G_{m_q} is the gain of the antenna m_q. h_{m_i} and h_{m_q} is the height of m_i and m_q antennas, respectively. h_{k_j} and G_{k_j} are the height and gain of k_j antenna. $d_{m_i k_j}$ is the distance of the desired signal, and $d_{m_q k_j}$ is the distance of the interfering signal; these are computed by Equation (4). The UAV's altitude is a crucial parameter embedded in the two-ray model, directly impacting the received signal strength. This approach enables the evaluation of signal propagation within a simplified 2D framework, effectively incorporating altitude considerations while avoiding the added complexity and computational demands of a full 3D model.

The two-ray and Rayleigh channel models represent a realistic model of a region after a natural disaster. A multipath fading channel is considered appropriate for this network model given that under the circumstances of a natural disaster, several scatters are expected to be encountered, either caused by debris, weather conditions, or changes in the original infrastructure. Therefore, it is expected that the transmitted signals will travel along different paths, each of random length, thus giving place to the multipath fading channel.

Therefore, the set of CMUs that ABSs may allocate a radio channel is given by:

$$A_i = \{a_j | k_j \in K \; and \; k_j \; satisfies \; the \; Equations \; (1), (2), (3)\} \quad (12)$$

where the ABS in the location m_i will assign a voice channel to the items of A_i through the channel assignment process. In this process, a_j becomes a served mobile user (SMU) only if:

$$success_{a_j} = \begin{cases} 1, & \text{if } a_j \text{ has a channel to transmit} \\ & \text{and it uses it during a time period} \\ 0, & \text{otherwise} \end{cases} \quad (13)$$

where $success_{a_j} = 1$ means that the a_j finishes its call within the evaluation time. Otherwise, the a_j is blocked (i.e., $success_{a_j} = 0$). Then, the set of SMUs is given by:

$$U_i = \{u_j | a_j \in A_i \; and \; success_{a_j} = 1\} \quad (14)$$

Therefore, the total number of SMUs properly attended (i.e., successful voice services) that provide the locations of the available ABSs is given by:

$$\Gamma = |\bigcup_{i=1}^{|M|} U_i| \tag{15}$$

In this paper, we evaluate the network performance by calculating the probability of successful voice service that provides the locations of the available ABSs. It is given by:

$$P(M) = \frac{\Gamma}{|K|} \tag{16}$$

where $|K|$ is the cardinality of the set K (the number of RMUs in the snapshot); and its value follows a Poisson distribution, and it depends on the average number of calls generated in the system, that is:

$$Q = \frac{A * 60}{T} \tag{17}$$

where A is the traffic intensity (Erlangs) of the system. T is the average time duration for a call in minutes.

We also calculated the total blocking probability P_{BT}, for each evaluated snapshot t_n. The P_{BT} metric is a performance measure for mobile communication systems, quantifying the network's ability to efficiently manage connection requests (calls) until the user completes their call. We make the assumption that the RMUs do not experience mobility, so we do not consider handover interruptions. Additionally, we assume that all call requests always outnumber the available channels, resulting in the continuous occupation of available channels in every snapshot. Furthermore, we maintain the assumption that link conditions remain stable and constant throughout the entire duration of the snapshot. In this work, the P_{BT} metric encompasses two blocking probabilities: the blocking probability due to coverage, denoted as P_{BC}, and the blocking probability due to spectral resources, denoted as P_{BR}. The P_{BT} is calculated as follows:

$$P_{BT} = P_{BC} + P_{BR} \tag{18}$$

where

$$P_{BC} = P_R | P_{OC} \tag{19}$$

$$P_{BR} = (P_R \cap P_{NA}) | P_{IC} \tag{20}$$

where P_{BR} represents the call request probability, and P_{OC} represents the user-out-of-coverage probability. On the other hand, P_{NA} indicates the probability of non-assignment and P_{IC} accounts for the user-in-coverage probability. Overall, P_{BC} occurs when an RMU is located outside the coverage zone of the ABS, while P_{BR} occurs due to a shortage of available communication channels.

2.3. Optimization model

Our objective is to find locations of the ABSs that provide the maximum probability of successful voice service in the disaster zone. Then, the problem can be formulated as follows:

$$Maximize\ P(M) = \frac{\Gamma}{|K|} \tag{21}$$

Subject to:

$$x_{min} \leq x_i \leq x_{max} \tag{22}$$

$$y_{min} \leq y_i \leq y_{max} \tag{23}$$

Equation (21) is the objective function (OF) that evaluates the set M that has the geographic coordinates of the ABSs. The value obtained in the OF indicates the probability of successful voice service the set of ABSs offers. The optimal expected value of the OF is one, meaning that M covers all RMUs. OF deals with feasible and infeasible individuals. In this paper, a feasible individual fulfills the mathematical iniquities (22) and (23). The iniquities (22) and (23) indicate that the m_i must not leave the bounds of the affected zone. These bounds are limited by x_{min} and x_{max} for latitude and by y_{min} and y_{max} for longitude.

On the other hand, we apply the death penalty method as a constraint-handling method to deal with infeasible individuals. This method of eliminating infeasible solutions is a well-accepted constraint-handling method in many evolutionary techniques. The death penalty method rejects individuals who do not comply with any of the constraints, and no information is extracted [27], that is:

$$P(M) = \begin{cases} \frac{\Gamma}{|K|}, & \text{when } M \text{ is feasible individual} \\ 0, & \text{when } M \text{ is infeasible individual} \end{cases} \tag{24}$$

3. (1+1)-Evolution Strategy

The problem is positioning each available ABS in the disaster zone to maximize the probability of successful voice services for mobile users. A (1+1)-ES algorithm can tackle the above, providing suitable solutions. It is an optimization metaheuristic that emphasizes the mutation and provides a self-adaptation mechanism under such an operator. Specifically, we applied the (1+1)-ES algorithm with a one-fifth success rule [10]. Using the one-fifth success rule, it uses an evolution loop in which a parent generates a single offspring. The one-fifth success rule adapts the step-size σ to mutate the offspring.

In this work, we represented an individual as S, as shown in Figure 3. It contains each ABS's latitude and longitude coordinates and one σ value. σ is the parameter that influences the mutation. In the real world, S provides the locations that ABSs will take inside the affected area. The affected area will have MUs (blue users), RMUs (yellow users), CMUs (red users), and SMUs (green users).

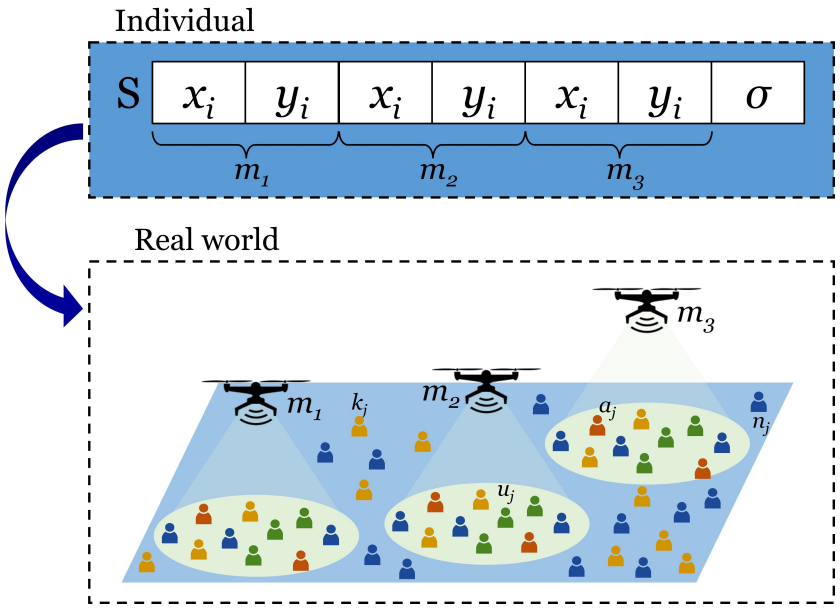

Figure 3: Representation of an individual in the (1+1)-ES algorithm.

The evaluation begins by generating a snapshot of the disaster zone, i.e., loading the geographic locations of MUs and randomly selecting RMUs ac-

cording to a uniform distribution. After, the (1+1)-ES takes the snapshot as an input and processes it according to Algorithm 1. In the initialization phase from STEP 1 to STEP 2, the archive of successful mutations A is created, and the success rate p_s is set to zero. Next, in STEP 3, the iteration counter variable t is set to zero. STEP 4 initializes the individual S. It consists of setting the initial value of σ and randomly generating the geographic positions of the ABSs. These locations follow a uniform normal distribution. They range from x_{min} to x_{max} in latitude and for longitude from y_{min} to y_{max}. Subsequently, STEP 5 sets to S as the parent S_p. In STEP 6, the fitness value is computed by following the process shown in Figure 4, and its value is stored in Fx_p. Here, the ABSs locations of S_p are evaluated in the OF as described in Section 3.1. The evolution loop begins in STEP 7. In STEP 9, an offspring S_o is created by adding to S_p a multivariate normal distribution $\mathcal{N}(0, I)$ with mean vector 0 and variance-covariance matrix. The offspring S_o recently created is evaluated in the OF, following the process described in Section 3.1, and its fitness is stored in Fx_o. From STEP 11 to STEP 17, the fittest individual between parent and offspring is selected. A success case is achieved if the offspring fitness value Fx_o is better than the parent fitness value Fx_p. Therefore, the offspring S_o becomes the parent S_p in the next iteration. The archive A stores that success case, i.e., $\#successes$ increases to one unit. Otherwise, a failure case occurs if the parent fitness value Fx_p is better than the offspring fitness value Fx_o. The above is stored in A, and $\#failures$ increases its counter in one unit. Hence, the parent S_p is kept for the next iteration. After that, the 1/5-success rule for step size adaptation σ is applied from STEP 18 to STEP 22. To so do, during a given number of iterations z, the step size σ is adapted. The 1/5-success rule states that the step size σ does not change if the success rate p_s equals 1/5, but if the success rate p_s falls below 1/5, the step size σ is reduced. On the other hand, the step size σ is increased if p_s grows above 1/5. Then, in STEP 23, the step size σ is updated. The evolution process finishes when the number of iterations T_{max} is reached. Finally, the (1+1)-ES algorithm finds the fittest individual that locates the ABSs to achieve the maximum probability of successful voice services.

3.1. Objective function evaluation

The process to obtain the fitness of the S_p and the S_o is shown in Figure 4. It begins by taking as input, the geographic locations of the ABSs along with the geographic locations of the RMUs. We verify the geographic locations of

Algorithm 1: (1+1)-ES

Data: The individual S, the step-size initial σ, the step size adaptation z, the stop condition T_{max}
Result: The best individual S

Initialize archive A for storing successful mutations;
$p_s = 0$;
$t = 0$;
Initialize individual S;
$S_p = S$;
$Fx_p = P(S_p)$;
while $t < T_{max}$ **do**
  $t = t + 1$;
  $S_o = S_p + \sigma \cdot \mathcal{N}(0, I)$; `/* · is a dot product */`
  $Fx_o = P(S_o)$;
  if $Fx_o > Fx_p$ **then**
    $S_p = S_o$;
    $Fx_p = Fx_o$;
    store success in A;
  else
    store failure in A;
  end
  if $t \mod z = 0$ **then**
    get $\#successes$ and $\#failures$ from at most $10z$ entries in A;
    $p_s = \frac{\#successes}{\#successes + \#failures}$;
    $$\sigma' = \begin{cases} \sigma * \text{c} & \text{if } p_s < 1/5 \\ \sigma \div \text{c} & \text{if } p_s > 1/5 \\ \sigma & \text{if } p_s = 1/5 \end{cases} ;$$
  end
  $\sigma = \sigma'$;
end

the ABSs, considering the Equations (22) and (23). The proposed solution is infeasible if any geographic coordinate of the available ABSs does not fulfill the constraints above. In this case, the individual's fitness is set to zero as Equation (24) indicates. Otherwise, if the solution is feasible, its fitness

is obtained through the snapshot-network evaluation process comprising the ABSs and channel assignments. The ABSs assignment process uses the locations of the RMUs and the verified locations of the S_p or the S_o to determine the CMUs. To do so, the RMU is within the coverage radius of some i-th ABS, i.e., the RMU fulfills the Equation (1). Next, the ABSs assignment process validates that the RMU is linked to a single ABSs by verifying the Equation (2). If the RMU approves the above conditions, the SINR is computed for the RMU as indicated in Equation (3). When the RMU achieves the Equations (1), (2), and (3), it becomes a CMU which is stored in the set A_i. Consequently, the ABS in the m_i position can assign its channels pool to the CMUs stored in A_i.

After that, the channel assignment process starts. It assigns channels to the CMUs linked to A_i. Then, A_i is an input to the channel assignment process. This process begins treating A_i as a first-in-first-out (FIFO) queue of the i-th ABS. $time_i$ stores the voice call duration for each CMU in A_i considering the CMU's order has in A_i. Hence, $time_i$ is a FIFO queue too. The voice call duration follows an exponential distribution. Next, the evaluation time of channel assignment (t_s) initializes at zero. This evaluation is a loop lasting 60 iterations. An iteration in the channel assignment evaluation is one minute in the system. The evaluation loop begins by checking if a CMU is in the queue A_i; if this is true, the channel assignment process verifies if the i-th ABS has an available channel inside its channel pool. If an available channel exists, the ABS assigns the channel to the CMU in the queue A_i and takes its voice call duration from $time_i$. It means the CMU will begin its call. Subsequently, the CMU and its channel occupation time are queued from A_i and $time_i$, respectively. Once A_i hasn't CMUs in the queue, or the ABS has all its channels occupied, the voice call duration of each CMU connected decreases by one unit. Afterward, the channel assignment process checks if there are calls finished. A call is finished when the counter of the occupation channel time of the CMU is zero. If so, the CMUs become SMUs, i.e., the CMUs have successfully completed their calls. The channels previously used by those CMUs return to the channel pool of the ABS that attended them. Then, the evaluation time of the snapshot increases in one unit. In the case there are no calls finished, the evaluation time of channel assignment increases too. After the 60 iterations, the snapshot evaluation time finishes, and the total of SMUs is calculated. Finally, the individual's fitness is computed using Equation (21).)

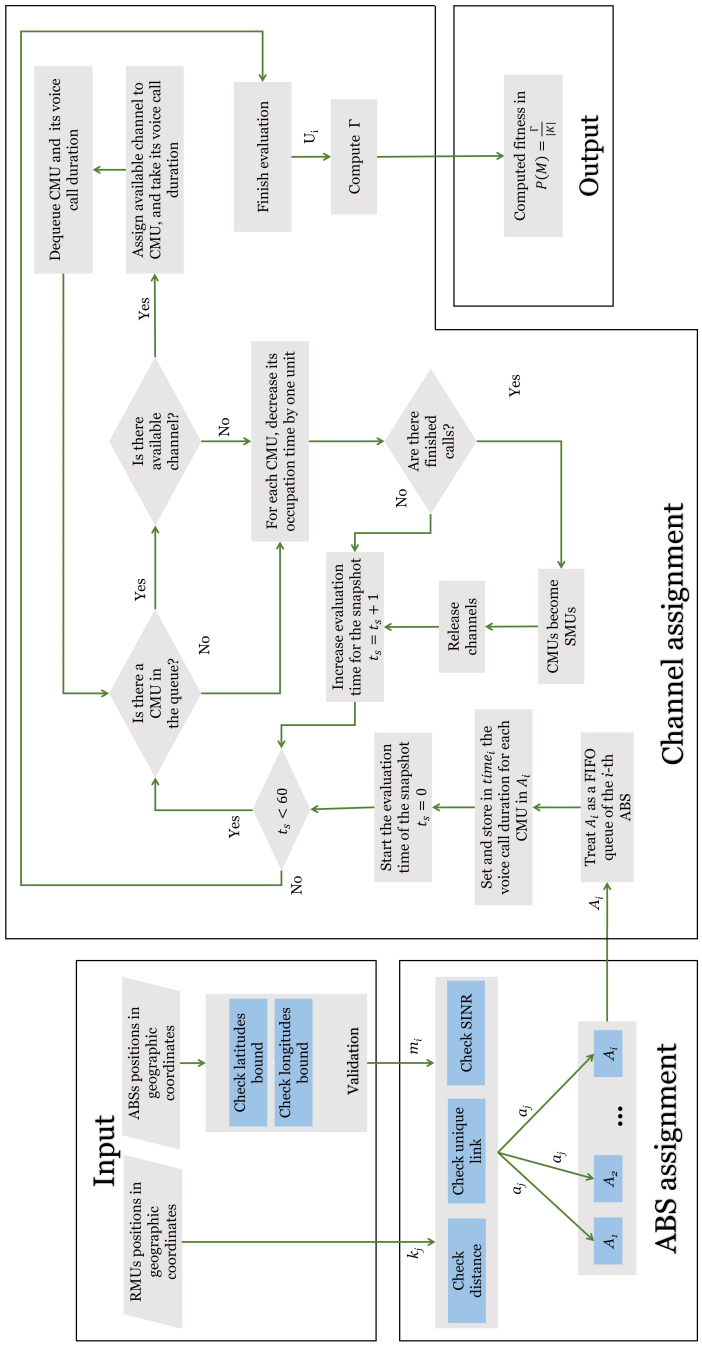

Figure 4: Snapshot-network evaluation to obtain the individual's fitness value.

4. Simulation Results

In this section, we present the simulation results obtained from the evaluation of our optimization model using the (1+1)-ES algorithm. We provide details on the parameters used in our computer simulations and describe the experiments we conducted. Our analysis focuses on assessing the performance of the (1+1)-ES algorithm in terms of the probability of successful voice services. Additionally, we analyze the total blocking probability to gain a comprehensive understanding of the system's behavior. Finally, we discuss the impact of different configurations of the (1+1)-ES algorithm on the evaluation time.

4.1. Simulation parameters

Table 3 shows the parameters in the simulation scenario. We consider a 12 km x 12 km disaster area corresponding to the town of Tula in Hidalgo, Mexico, with 29 390 inhabitants [28]. From that whole population, we only consider 19 819 MUs distributed within the affected area, i.e., $|N|$ = 19 819. Also, we assume the emergency services have four ABS to providing communication services, that is $|M|$ =4. The average number of RMUs per ABS (Q) is computed by Equation (17). It considers the traffic intensity A in 56.11 Erlangs (70 channels), an outage probability of 1%, and the average time duration of an emergency call T at three minutes as reported in [29]. Therefore, the average number RMUs in the affected area is given by the available number ABS ($|M| = 4$) and the average number RMUs per ABS ($Q = 1\ 123$).

The parameters used in the network are chosen to enable the voice service of an LTE network. We considered the carrier frequency band of 700 MHz, and all ABSs transmit at the same power level P_{tx} (95 dB). LTE supports a maximum transmit power of 100 dB [30]. It is important to note that we assumed that the available ABSs are low-altitude platforms (LAPs). LAPs are usually employed to enhance cellular communications due to their cost-effectiveness compared to high-altitude platforms (HAPs). LAPs allow fast deployment capabilities and enable short-range LoS communication links, which can significantly improve communication performance [31]. Therefore, we set the altitudes of all the ABSs (h_{m_i} and h_{m_q}) at 122 m according to [32].

Parameters	Value
Disaster zone	12 km x 12 km
Number of MUs	19,819
Number of ABSs	4
Average number RMUs in the affected area	4,492
Carrier frequency	700 MHz
Transmitter power ABS P_{tx}	95 dB
ABSs altitude h_{m_i} and h_{m_q}	122 m
ABS antenna gain G_{m_i} and G_{m_q}	10 dB
RMUs altitude h_{k_j}	1.5 m
RMU antenna gain G_{k_j}	3 dB

Table 3: Parameters of the affected area and network used in the simulation.

4.2. Experimental results

We evaluated the optimization model on the simulation environment described in Section 2. To do so, we applied the (1+1)-ES algorithm. We designed four experiments to determine the best performance of the (1+1)-ES algorithm on the problem of the location of ABS for scenarios where communication is interrupted. Table 4 shows the parameters in the carried-out experiments. On the other hand, an optimization algorithm has different parameters that need to be set up with specific values. These parameters will impact the quality of the solutions; hence is necessary to select values that allow the best performance of the optimization algorithm. Parameter setting is a non-trivial process and requires knowing the parameters' effect on the problem. In this sense, the (1+1)-ES performance is influenced by σ and z parameters. The step-size σ gives the search scale and generates a perturbation on the multivariate random vector causing the mutation in the solutions. σ is adapted at each number of iterations z of the algorithm and according to success rate p_s. z defines how many iterations must elapse to adapt σ. Then, in Table 4, the first column is the experiment's names. The second column is the initial value of step size σ used at each experiment. The step size σ (in decimal degrees) is related to the displacement scale of each ABS. Since the largest side of the affected area is equal to 12 km, then the maximum displacement scale is set to 0.1 decimal degrees in the individual. In Table 4, the second column shows the displacements in the base-10 num-

ber system, indicated within parentheses. The third column is the z value. This value is set to ten for the four experiments because, in previous tests, we observed that for z=5, the algorithm converged too early and lost the ability to explore the solutions space. On the other hand, from the previous study for z=20, we detected that the algorithm delayed the convergence affecting the delivery time of a solution; this value allowed the exploration of the solutions space. Finally, from a prior study of z=10, we noticed that the algorithm obtained the balance between exploitation and exploration since it offered high-quality solutions.

Experiment	**Step size σ**	**Value z**
(1+1)-ES_1	0.1 (12 km)	10
(1+1)-ES_2	0.01 (1.2 km)	10
(1+1)-ES_3	0.001 (0.12 km)	10
(1+1)-ES_4	0.0001 (0.012 km)	10

Table 4: Values of the step size σ used in the four experiments to evaluate the performance of the (1+1)-ES.

The purpose of the four experiments described in Table 4 is to analyze the performance of the (1+1)-ES algorithm by modifying the displacement scale and determining which is more efficient in positioning ABSs in a bounded zone. 30 different network snapshots are evaluated at each experiment. Each network snapshot t_n considers the same MU positions and the same number of MUs ($|N|$=19,819). The number of RMUs is different in each network snapshot; it is given by a Poisson distribution with an average of 4,492 requests in the system. Different RMUs are selected to evaluate each network snapshot. The four experiments were carried out in Python programming language version 3.6 and were run on a Jetson TX2, with Ubuntu 18.04 LS operative system, 64-bit Denver 2 A57 CPUs, 8 GB 128-bit LPDDR4 58.4 GB/s, NVIDIA Pascal with 256 cores GPU.

Figure 5 shows the best solution obtained in the different network snapshots evaluated on (1+1)-ES for the different step sizes σ shown in Table 4. The best solution is the optimal combination of ABS locations found by (1+1)-ES; thus, those are the ABSs locations in the snapshot that should be deployed. Here, (1+1)-ES_3 experiment (σ=0.001) obtained the best performance; it provided solutions on average 6.5% higher than the general mean of all experiments, its evolution process generated the highest average num-

ber of successful cases (25.5 successful cases). A successful case is a feasible candidate solution (offspring) that exceeds the quality of a feasible candidate solution from the previously generated (parent). On the other hand, (1+1)-ES_4 experiment (σ=0.0001) obtained the worst performance because found solutions on average 14.6% lower than the overall general mean of tests. Moreover, it has the highest number of solutions at zero; a solution at zero indicates that the algorithm did not find feasible candidate solutions during its evolution. In the context of this work, finding feasible candidate solutions is essential because the algorithm is expected to ensure solutions that facilitate the efficient localization of ABSs, enabling first responders to establish communication with potential victims situated within the impacted area.

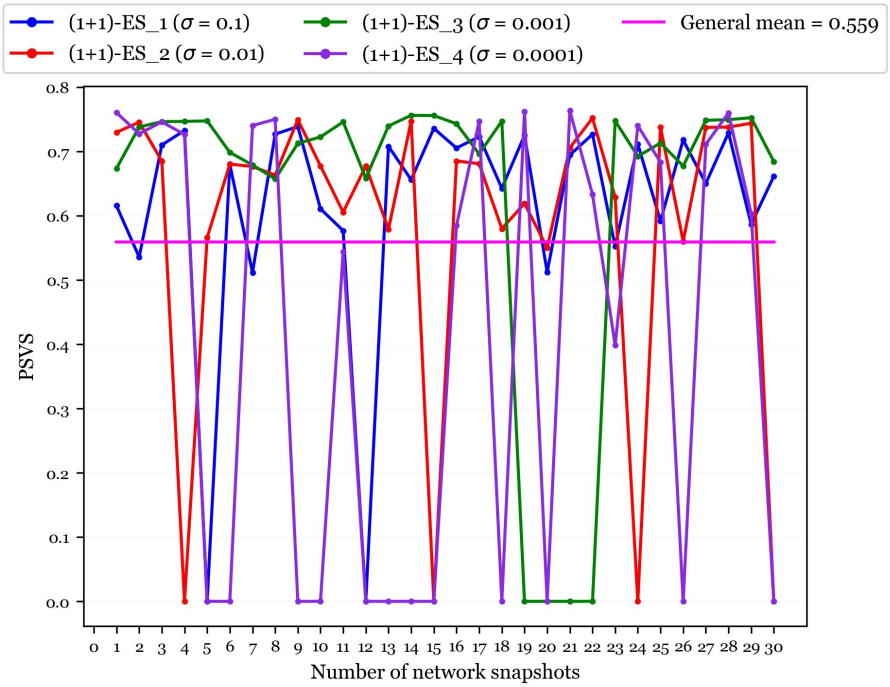

Figure 5: Best solutions delivered by (1+1)-ES. Solutions indicate the PSVS that the ABS positions provide.

Table 5 shows experimental results obtained by evaluating 30 network snapshots for each experimental design. The (1+1)-ES_1 (σ=0.1) experiment demonstrates its capability to find feasible solutions, reducing the probability of obtaining solutions at zero. However, it does not guarantee to achievement

of the highest quality solutions, as evidenced in the second column in Table 5. In the (1+1)-ES_2 (σ=0.01) and (1+1)-ES_3 (σ=0.001) experiments, both setups have the same ability to find feasible solutions and provide solutions of similar quality (see the second column). Nevertheless, on average (see the third column), (1+1)-ES_3 provides solutions 4% higher than (1+1)-ES_2. In contrast, the (1+1)-ES_4 (σ=0.0001) generated the best solution, achieving a PSVS of 0.76357. However, it also obtained the highest probability of failing to find a solution (0.4). This means that 40% of the time the algorithm did not find a solution. Based on these results, we suggested using the parameters of the (1+1)-ES_3 experiment. Although it does not provide the best solution, this setup provides the highest probability of obtaining PSVS superior at 0.6. In other words, the configuration of the (1+1)-ES_3 experiment indicates that the positions of ABSs can offer a 62% probability of establishing a successful network connection for users or emergency operators.

Experiment	**Best solution**	**Mean**	**POS $\geq$ 0.60**	**POS = 0**
(1+1)-ES_1	0.73879	0.61570	0.70	**0.067**
(1+1)-ES_2	0.75208	0.58343	0.70	0.133
(1+1)-ES_3	0.75634	**0.62440**	**0.867**	0.133
(1+1)-ES_4	**0.76357**	0.41275	0.50	0.40

Table 5: Experimental results obtained by the evaluation of 30 network snapshots of each experiment. POS is the probability of obtaining a solution.

To analyze how σ influences the algorithm's performance, the best solution found in each experiment was plotted in Figure 6. Specifically, Figures 6a, 6c, 6e and 6g show the PSVS values of the feasible candidate solutions and their corresponding σ values observed during the evolutionary process of the (1+1)-ES. We observed how the initial value of σ influences the search for the solutions in the algorithm. In Figure 6a of the (1+1)-ES_1 experiment (initial σ=0.1), the algorithm explores the solutions space but does not emphasize the exploitation process. In the (1+1)-ES_3 (initial σ=0.001), we observed a balance between the exploration and exploitation processes of the solutions space (see Figure 6e). In the case of the (1+1)-ES_4 experiment (see Figure 6g), where the initial step size (σ) is set to 0.0001, the algorithm exhibits a tendency to prioritize exploitation over exploration during the early iterations. This bias towards exploitation can result in premature conver-

gence. We also observed that; σ always decreases with the pass of iterations, that is, the probability of obtaining a successful solution is lower than 0.20, as the one-fifth success rule indicates it. In general, (1+1)-ES explores the search space when σ takes values from 0.1 (maximum displacement scale) to 2.33×10^{-6} approximately and exploits the displacement space when σ takes a value in the range from 2.33×10^{-6} to 1.85×10^{-7}. Figures 6b, 6d, 6f, and 6h show the displacements of each ABS by experimental design in the evolution of the best solution of each experiment. We observed that as the displacements are affected by the σ value, σ decreases, and the distance displacement between feasible candidate solutions is reduced. Comparing the displacements with the σ behavior, the (1+1)-ES exploits, on average, in distances less than 0.200 km, and it explores otherwise.

We analyzed the function calls to both the penalty and objective functions. Figure 7 shows the average number of calls made to each experiment's penalty and objective functions. Notably, we identified a clear correlation between the initial step size, denoted as σ, and the frequency of calls to these functions. As σ decreases, we observed an increase in the number of calls to the objective function, accompanied by a decrease in calls to the penalty function. This phenomenon can be attributed to the significant influence of the initial value of σ on the starting point in the algorithm's evolution process. Specifically, in the ES-(1+1)_1 experiment, its evolutionary process begins by perturbing the mutation operator with 0.1, equivalent to a distance of 12 km, causing the algorithm to take an average of 246 iterations to find a space with feasible solutions. In contrast, the (1+1)-ES_2 experiment started its evolution process with a perturbation of 0.01, equivalent to a distance of 1.2 km. It required an average of 118 iterations to find a space with feasible solutions. Moving to (1+1)-ES_3, it initiated its evolution process with a perturbation of 0.001, equivalent to a distance of 0.12 km. On average, it took only 15 iterations to find a space with feasible solutions. Finally, the ES-(1+1)_4 experiment initiated its evolution process with a perturbation of 0.0001, equivalent to a distance of 0.012 km, resulting in an average of just 8 iterations to find a space with feasible solutions. The above indicates that the algorithm faces a more challenging task when initializing its evolution process with a distance of 12 km (0.1) compared to a starting distance of 0.012 km (0.012).

On the other hand, comparing Table 5 and Figure 7, we observed that the initial value of σ has an impact on the quality of solutions and the search process. (1+1)-ES_1 obtained the fewest calls to the objective function but

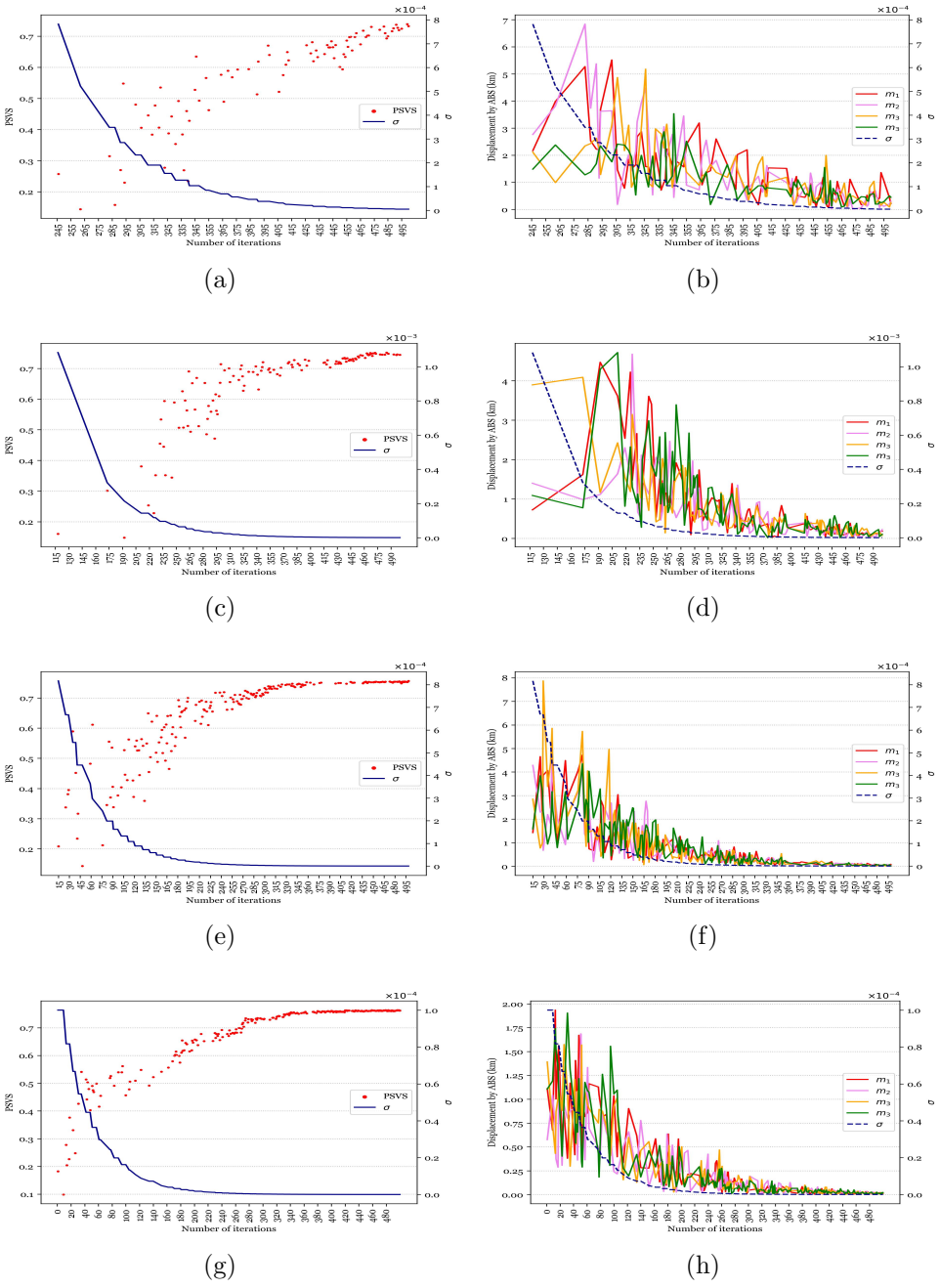

Figure 6: The behavior of the evolution process of the best solution found at each experiment.

produced the lowest-quality solution (0.73879) due to its limited exploitation process. In contrast, (1+1)-ES_2, called the objective function 122 times during its search but failed to effectively exploit the solution space. As for (1+1)-ES_3, on average, it called the objective function 183 times, thus achieving the highest average in the PSVS (0.6244) and striking a balance between exploitation and exploration processes. Finally, (1+1)-ES_4 on average called the objective function more times (200) and delivered the highest-quality solution (0.76357) but prioritized exploitation over exploration in the search process. Therefore, as the number of calls to the objective function increases, the algorithm gains the capacity to exploit the solution space more effectively. Importantly, the number of calls to the objective function also influences the evaluation time. On average, (1+1)-ES_4 required 1,058 seconds to return a solution, while (1+1)-ES_1 delivered a solution in an average time of 475 seconds. (1+1)-ES_2 and (1+1)-ES_3 returned solutions in 672 seconds and 979 seconds, respectively. Given the critical role of evaluation time in our work, these findings are of utmost significance.

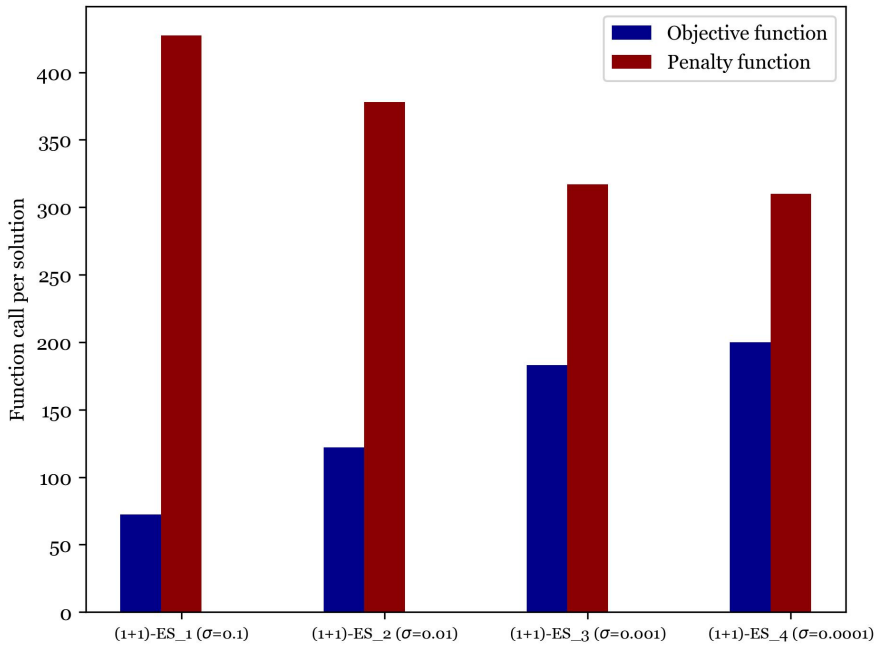

Figure 7: Average number of evaluations to a solution (penalty function and objective function).

We also analyze the total blocking probability obtained from the different network snapshots evaluated on the (1+1)-ES algorithm. The results are summarized in Table 6. The first column contains the experiment names, while the second column shows the initial average total blocking probability, denoted as P_{BI}. This value is derived from the first random candidate solution generated by the algorithm, specifically, the first parent generated in each network snapshot evaluation. If there are any shared RMUs in the coverage of the ABSs, then P_{BI} is set to 1, because our model does not consider a handover strategy. Otherwise, P_{BI} is calculated using Equation (18). We also provide the averages of the blocking probability due to coverage (P_{BC}), the blocking probability due to spectral resources (P_{BR}), and the total blocking probability (P_{BT}) resulting from the locations of ABSs that provide the maximum PSVS in each network snapshot evaluated. In general, P_{BC} is calculated using Equation (19), which includes voice services denied to RMUs located outside the coverage radius of the ABSs. Each ABS has a coverage radius of two km. P_{BR} is computed with Equation (20), which considers the voice services denied to CMUs due to channel unavailability and those denied because they could not complete their voice calls during the network snapshot evaluation process. Finally, in the last column, we report the average reduction percentage of the blocking probability achieved between the first solution generated by the (1+1)-ES algorithm and after its implementation.

In Table 6, we observed that the average value of the P_{BI} in all experiments exceeded 0.9. This trend can be primarily attributed to the fact that, in 85% of the cases, the (1+1)-ES algorithm was initiated with solutions where some RMUs were shared within the coverage radius of two or more ABS. An example of this is shown in Figure 8a. Notably, the (1+1)-ES_3 experiment achieved the highest P_{BI} value due to having the highest number of parents with a P_{BI} value of 1. We also noted that the (1+1)-ES_4 experiment had the highest values for P_{BC}, P_{BR}, and P_{BT}. In this case, the algorithm either failed to find a solution, or the ABSs shared RMUs within their coverages. Consequently, P_{BC}, P_{BR}, and P_{BT} were set to 1. On the other hand, the (1+1)-ES_1 experiment exhibited the lowest values for P_{BC}, P_{BR}, and P_{BT}. This outcome stems from the algorithm finding feasible solutions in 93% of the cases, enabling us to obtain P_{BT} value in the snapshot evaluated. However, the (1+1)-ES_3 experiment achieved the highest reduction percentage due to several factors: it had the highest PSVS compared to (1+1)-ES_1, (1+1)-ES_2, and (1+1)-ES_4; its search process struck a balance between exploration and exploitation; and had an 83% probability of

obtaining feasible solutions in the evolution process.

Experiment	**Mean**				**Reduction percentage**
	P_{BI}	P_{BC}	P_{BR}	P_{BT}	
(1+1)-ES_1	0.9046	0.27737	0.27822	0.48892	41.6%
(1+1)-ES_2	0.9089	0.32789	0.33007	0.52423	38.5%
(1+1)-ES_3	0.9410	0.32625	0.32892	0.52184	41.9%
(1+1)-ES_4	0.9074	0.53352	0.53666	0.67018	23.7%

Table 6: Experimental results of total blocking probability.

In emergency situations, the ABSs and spectral resources are often limited. Therefore, depending on random ABS placement may not be the most efficient approach. This is because spectral resources may not be optimally utilized when ABSs are not strategically positioned in areas where people need communication services. Efficiently locating available ABSs is crucial to ensure the effective utilization of spectral resources. Therefore, based on the results we have obtained, we recommend utilizing the (1+1)-ES_3 experiment configuration. This configuration has the highest probability of achieving a PSVS superior to 0.6, and its evolution process strikes a balance between exploration and exploitation and produces the highest reduction percentage in the P_{BT}. Hence, Figure 8 illustrates the best solution obtained in the (1+1)-ES_3 experiment. Figure 8a shows the initial solution generated by the algorithm; the initial positions of the available ABSs share RMUs within the coverage of the ABSs. Consequently, the algorithm assigns a PSVS of zero to these initial positions. This approach aligns with our model's objective, which aims to efficiently use the available resources. Also, it provides some degree of control over the coverage overlap of the ABSs. In Figure 8a, the blue points are the MUs, and the RMUs are the yellow points. The ABSs are the color triangles, and the circles in the same color as the triangles depict their coverage radius ABS. Figure 8b shows the search process of the experiment. As the algorithm evolves, the positions of the ABSs can shift due to the exploit and explore processes. The initial ABS positions are the color triangles, the search process is the color points, and the final ABS positions are the color crosses. We observed that the algorithm searches the best locations for maximizing the probability of successful voice service. The best solution is illustrated in the real world in Figure 8c; the positions of the ABSs are the aircraft marks, the coverage of each ABS is a dark red circle,

the RMUs locations are the yellow marks, the green marks are SMUs (the users successfully served by an ABS). It is crucial to ensure that the ABSs are optimally positioned for maximum PSVS. As observed in Figure 8c, the ABSs are located in areas with more RMUs, which highlights the significance of an optimized positioning strategy.

A similar study in [15] reported a mobile coverage ratio up to nearly 94% to 96% for ten ABSs (52 to 53 out of 55 mobile users) in a simulation area of 200 m x 200 m. Our simulation stresses network resources beyond the standard setting and uses the ABSs resources more efficiently since our approach can cover a wider area with a high concentration of mobile users using only four ABSs. We achieved an average coverage of 62% (3219 out of 4462 mobile users) in a 12 km x 12 km area.

5. Conclusions

The experimental results demonstrated the effectiveness of the proposed model in locating ABSs within affected areas, specifically targeting regions where a significant number of users attempt to access the network to make calls. The results obtained from the (1+1)-ES algorithm indicate that when initialized with a large step size ($\sigma = 0.1$), it requires more effort to find feasible solutions within the search space. In contrast, using a smaller step size ($\sigma = 0.001$) demands less effort. σ perturbs the mutation operator, causing the (1+1)-ES to explore the search space with larger step sizes (from 0.1 to 2.33×10^{-6}) and exploit the search solutions with smaller step sizes (from 2.33×10^{-6} to 1.85×10^{-7}). Overall, the initial step size σ significantly impacts the performance and efficiency of the (1+1)-ES algorithm. Therefore, when parameters are properly calibrated, the (1+1)-ES can determine the positions of ABSs.

On the other hand, when comparing the total blocking probability delivered by a random positioning of the ABS against the total blocking probability obtained by positioning the ABS using the (1+1)-ES algorithm, a significant improvement is observed. On average, the use of the (1+1)-ES algorithm reduced the total blocking probability by 36%. Nevertheless, it is important to note that there remains an average total blocking probability of 0.55. This means that there is a 55% chance that a call request will be blocked due to insufficient resources, including ABSs or channels. This limitation can be attributed to our network model's inability to handle call requests that fall within the coverage areas of two or more ABSs. However,

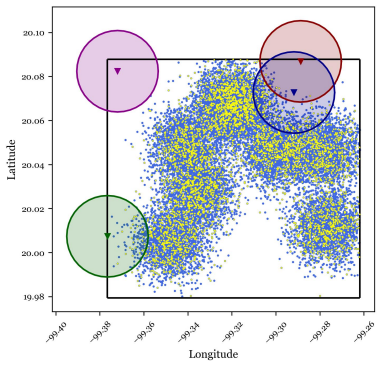

(a) Initial

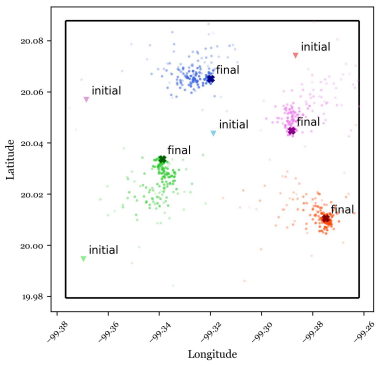

(b) Evolution

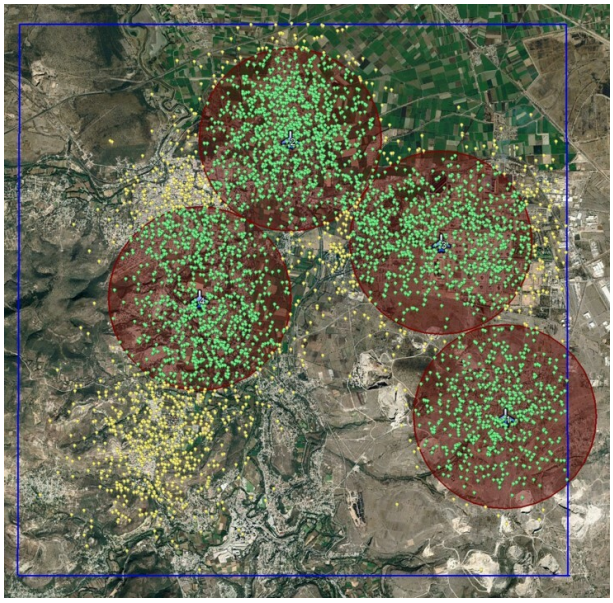

(c) Final

Figure 8: Best solution found in the experiment (1+1)-ES_3: (a) represents the initial solution generated by the algorithm, (b) shows the evolution process of the algorithm, and (c) represents the best solution found by the algorithm.

this issue can be resolved by implementing an allocation strategy for such cases. Additionally, the blocking probability can be reduced by incorporating more ABSs, expanding the coverage radius, or considering a heterogeneous network architecture—these are tasks we plan to address in the future.

In future work, we plan to include a constraint for the deletion overlaps in ABSs coverage. Additionally, we will explore methods to enhance network performance, which could involve exploring channel assignment strategies or channel reuse techniques. Our aim is to reduce the probability of service blocking and increase the likelihood of successful voice service completion, leveraging the available spectral resources. We will tune the evolution strategy parameters using reinforcement learning methods. In doing so, we aim to attain the best algorithmic performance. Furthermore, in emergency scenarios, response times are critical. Therefore, we will explore implementing our proposed model in parallel computing to decrease execution times.

References

[1] R. Singh, K. Ram, C. Yadav, A. R. Siddiqui, Climate change, disaster and adaptations: Human responses to ecological changes, in: Climate Change, Disaster and Adaptations: Contextualising Human Responses to Ecological Change, Springer, 2022, pp. 121–130.

[2] H. J. Caldera, S. C. Wirasinghe, A universal severity classification for natural disasters, Natural Hazards 111 (2) (2022) 1533–1573. doi:10.1007/s11069-021-05106-9.

[3] R. Shahzadi, M. Ali, H. Z. Khan, M. Naeem, Uav assisted 5g and beyond wireless networks: A survey, Journal of Network and Computer Applications 189 (2021) 103114. doi:https://doi.org/10.1016/j.jnca.2021.103114.

[4] S. Biswas, R. Muttangi, H. Patel, S. Prince, Edge ai based autonomous uav for emergency network deployment: A study towards search and rescue missions, in: 2022 International Conference on Wireless Communications Signal Processing and Networking (WiSPNET), 2022, pp. 268–272. doi:10.1109/WiSPNET54241.2022.9767139.

[5] AT&T, Flying cow connects puerto rico, AT&T Blog (2017).
URL https://about.att.com/inside_connections_blog/flying_cow_puertori

[6] N. Parvaresh, B. Kantarci, Deep q-learning-enabled deployment of aerial base stations in the presence of mobile users, in: Proceedings of the 20th ACM International Symposium on Mobility Management and Wireless Access, MobiWac '22, Association for Computing Machinery, New York, NY, USA, 2022, p. 73–80. doi:10.1145/3551660.3560909.

[7] X. Zhong, Y. Huo, X. Dong, Z. Liang, Qos-compliant 3-d deployment optimization strategy for uav base stations, IEEE Systems Journal 15 (2) (2021) 1795–1803. doi:10.1109/JSYST.2020.3015428.

[8] R. Gao, X. Wang, Rapid deployment method for multi-scene uav base stations for disaster emergency communications, Applied Sciences 13 (19) (2023). doi:10.3390/app131910723.
URL https://www.mdpi.com/2076-3417/13/19/10723

[9] M. Alzenad, A. El-Keyi, F. Lagum, H. Yanikomeroglu, 3-d placement of an unmanned aerial vehicle base station (uav-bs) for energy-efficient maximal coverage, IEEE Wireless Communications Letters 6 (4) (2017) 434–437. doi:10.1109/LWC.2017.2700840.

[10] T. Bäck, C. Foussette, P. Krause, Contemporary Evolution Strategies, Natural Computing Series, Springer, 2013. doi:10.1007/978-3-642-40137-4.
URL http://link.springer.com/10.1007/978-3-642-40137-4

[11] J. Kacprzyk, W. Pedrycz, Springer handbook of computational intelligence, Springer, 2015.

[12] S. H. Alsamhi, A. V. Shvetsov, S. Kumar, S. V. Shvetsova, M. A. Alhartomi, A. Hawbani, N. S. Rajput, S. Srivastava, A. Saif, V. O. Nyangaresi, Uav computing-assisted search and rescue mission framework for disaster and harsh environment mitigation, Drones 6 (7) (2022). doi:10.3390/drones6070154.

[13] N. U. Hasan, P. Valsalan, U. Farooq, I. Baig, On the recovery of terrestrial wireless network using cognitive uavs in the disaster area, International Journal of Advanced Computer Science and Applications 11 (4) (2020). doi:10.14569/IJACSA.2020.01104106.

[14] C. T. Cicek, H. Gultekin, B. Tavli, The location-allocation problem of drone base stations, Computers & Operations Research 111 (2019) 155–176. doi:https://doi.org/10.1016/j.cor.2019.06.010.

[15] Z. Zhao, P. Cumino, C. Esposito, M. Xiao, D. Rosário, T. Braun, E. Cerqueira, S. Sargento, Smart unmanned aerial vehicles as base stations placement to improve the mobile network operations, Computer Communications 181 (2022) 45–57. doi:https://doi.org/10.1016/j.comcom.2021.09.016.

[16] P. Q. Viet, D. Romero, Aerial base station placement: A tutorial introduction, IEEE Communications Magazine 60 (5) (2022) 44–49. doi:10.1109/MCOM.001.2100861.

[17] X. Liu, Y. Liu, Y. Chen, Reinforcement learning in multiple-uav networks: Deployment and movement design, IEEE Transactions on Vehicular Technology 68 (8) (2019) 8036–8049. doi:10.1109/TVT.2019.2922849.

[18] J. Li, D. Lu, G. Zhang, J. Tian, Y. Pang, Post-disaster unmanned aerial vehicle base station deployment method based on artificial bee colony algorithm, IEEE Access 7 (2019) 168327–168336. doi:10.1109/ACCESS.2019.2954332.

[19] A. U. Chaudhry, R. H. M. Hafez, Lmr and lte for public safety in 700MHz spectrum, Wireless Communications and Mobile Computing 2019, publisher: Hindawi (2019). doi:10.1155/2019/7810546.
URL https://doi.org/10.1155/2019/7810546

[20] H. ElSawy, E. Hossain, M. Haenggi, Stochastic geometry for modeling, analysis, and design of multi-tier and cognitive cellular wireless networks: A survey, IEEE Communications surveys & tutorials 15 (3) (2013) 996–1019.

[21] S. Bruhn, H. Pobloth, M. Schnell, B. Grill, J. Gibbs, L. Miao, K. Järvinen, L. Laaksonen, N. Harada, N. Naka, S. Ragot, S. Proust, T. Sanda, I. Varga, C. Greer, M. Jelínek, M. Xie, P. Usai, Standardization of the new 3gpp evs codec, in: 2015 IEEE International Conference on Acoustics, Speech and Signal Processing (ICASSP), 2015, pp. 5703–5707. doi:10.1109/ICASSP.2015.7179064.

[22] H. Mahmoud, N. Akkari, Shortest path calculation: a comparative study for location-based recommender system, in: 2016 world symposium on computer applications & research (WSCAR), IEEE, 2016, pp. 1–5.

[23] J. T. Penttinen, The LTE-advanced deployment handbook: the planning guidelines for the fourth generation networks, John Wiley & Sons, 2016.

[24] T. S. Rappaport, et al., Wireless communications: principles and practice, Vol. 2, Prentice-Hall PTR, 1996.

[25] A. Ranjan, B. Panigrahi, H. K. Rath, P. Misra, A. Simha, H. Sahu, A study on pathloss model for uav based urban disaster and emergency communication systems, in: 2018 Twenty Fourth National Conference on Communications (NCC), IEEE, 2018, pp. 1–6.

[26] A. Goldsmith, Wireless Communications, Cambridge University Press, 2005. doi:10.1017/CBO9780511841224.

[27] J. R. McDonnell, R. G. Reynolds, D. B. Fogel, A Survey of Constraint Handling Techniques in Evolutionary Computation Methods, Mit Press, 1995.

[28] INEGI, Censo de población y vivienda 2021, https://www.inegi.org.mx, access in February 2022 (Jan-Dic 2022).

[29] C. nacional de información, Estandarización de los servicios de llamadas de emergencia a través del número único armonizado 9-1-1 (nueve, uno, uno), https://www.gob.mx/911/documentos/norma-tecnica-para-la-estandarizacion-de-los-servicios-de-llamadas-de-emergencia-a-traves-del-numero-unico-armonizado-9-1-1 (January 2018).

[30] D. Tse, P. Viswanath, Fundamentals of wireless communication, Cambridge university press, 2005.

[31] A. Fotouhi, H. Qiang, M. Ding, M. Hassan, L. G. Giordano, A. Garcia-Rodriguez, J. Yuan, Survey on uav cellular communications: Practical aspects, standardization advancements, regulation, and security challenges, IEEE Communications Surveys & Tutorials 21 (4) (2019) 3417–3442. doi:10.1109/COMST.2019.2906228.

[32] M. Mozaffari, W. Saad, M. Bennis, Y.-H. Nam, M. Debbah, A tutorial on uavs for wireless networks: Applications, challenges, and open problems, IEEE Communications Surveys & Tutorials 21 (3) (2019) 2334–2360. doi:10.1109/COMST.2019.2902862.